ELSEVIER

q

Contents lists available at ScienceDirect

Earth and Planetary Science Letters

journal homepage: www.elsevier.com/locate/epsl



Europium anomalies in zircon: A signal of crustal depth?

Chris Yakymchuk ^{a,*}, Robert M. Holder ^b, Jillian Kendrick ^c, Jean-François Moyen ^d

- ^a Department of Earth and Environmental Sciences, University of Waterloo, Waterloo, Ontario N2L 3G1, Canada
- b Department of Earth and Environmental Sciences, University of Michigan, Ann Arbor, MI, 48109-1005, USA
- ^c Department of Earth and Planetary Sciences, McGill University, Montreal, Quebec H3A 0E8, Canada
- d Université de Lyon, Laboratoire Magmas et Volcans, UJM-UCA-CNRS-IRD, 23 rue Dr. Paul Michelon, 42023 Saint Etienne, France

ARTICLE INFO

Article history:
Received 2 May 2023
Received in revised form 15 August 2023
Accepted 13 September 2023
Available online xxxx
Editor: R. Hickey-Vargas

Keywords: zircon Europium anomaly paleodepth phase equilibrium modelling

ABSTRACT

Trace element concentrations and ratios in zircon provide important indicators of the petrological processes that operate in igneous and metamorphic systems. In granitoids, the compositions of zircon have been linked to the behaviour of garnet and plagioclase-pressure-sensitive minerals-in the source during partial melting. This has led to the proposal that Europium anomalies in detrital zircon are linked to the depth of crustal melting or magmatic differentiation and are a proxy for average crustal thickness. In addition to the mineral assemblage present during partial melting, Eu anomalies in zircon are also sensitive to redox conditions as well as magma evolution during extraction, ascent, and emplacement. Here we quantitatively model how rock type mineral assemblages, redox changes, and reaction sequences influence Eu anomalies of zircon in equilibrium with silicate melt. Partial melting of metasedimentary rocks and metabasites yields felsic to intermediate melts with a large range of Eu anomalies, which do not correlate simply with pressure (i.e. depth) of melting. Europium anomalies of zircon associated with partial melting of metasedimentary rocks are most sensitive to temperature whereas Eu anomalies associated with metabasite melting are controlled by plagioclase proportion-a function of pressure, temperature, and rock composition-as well as changes in oxygen fugacity. Furthermore, magmatic crystallization of granitoids can increase or decrease Eu anomalies in zircon from those of the initial (anatectic) melt. Therefore, Eu anomalies in zircon should not be used as a proxy for the crustal thickness or depth of melting but can be used to track the complex processes of metamorphism, partial melting, and magmatic differentiation in modern and ancient systems. Secular changes of Eu/Eu* from the zircon archive may reflect a change in thermal gradients of crustal melting or an increase in the reworking of sedimentary rocks over time.

© 2023 The Author(s). Published by Elsevier B.V. This is an open access article under the CC BY-NC license (http://creativecommons.org/licenses/by-nc/4.0/).

1. Introduction

Europium is an important rare earth element (REE) for understanding the long-term evolution of the continental crust because it is redox sensitive (Philpotts, 1970; Hinton and Upton, 1991; Ballard et al., 2002; Trail et al., 2012) and preferentially partitioned into feldspars as a divalent cation (e.g. Weill and Drake, 1973). Because of Eu enrichment in feldspars, whole-rock and accessory mineral Eu anomalies (Eu/Eu* = Eu_N / [Sm_N x Gd_N]^{0.5}; where the subscript $_{\rm N}$ denotes chondrite-normalized values) have been used to infer the behaviour of feldspars in igneous and metamorphic systems (e.g. Murali et al., 1983; Rubatto, 2002; Holder et al., 2020). For example, igneous whole-rock Eu anomalies have been used as a proxy for the depths of partial melting and magmatic

Trace element ratios of igneous rocks—such as Sr/Y—have also been used as a crustal thickness proxy (e.g. Chapman et al., 2015), which is somewhat analogous to using Eu/Eu* anomalies in zircon and suffers from the same limitation of reflecting only minimum crustal thickness. The petrological argument for using trace

https://doi.org/10.1016/j.epsl.2023.118405

0012-821X/© 2023 The Author(s). Published by Elsevier B.V. This is an open access article under the CC BY-NC license (http://creativecommons.org/licenses/by-nc/4.0/).

differentiation, because of the pressure-dependence of plagioclase stability (e.g. Rudnick, 1992). As a result of these previous observations and interpretations of Eu anomalies from whole-rock samples of and zircon from intermediate igneous rocks, detrital zircon Eu anomalies have been used to infer changes in the average thickness of crust in Earth's past (Tang et al., 2021). This extrapolation is, in itself, problematic: assuming Eu anomalies monitor the depth of melting, the only logical inference is that the crust in which this melting occurred was not thicker than the depth of melting. This is not always the case—post-orogenic terranes, for instance, commonly record melting in the shallow portions of an otherwise still thick crust. Thus, Eu/Eu* is, at best, a tracer of minimum crustal thickness, but does not inform on the actual thickness.

^{*} Corresponding author.

E-mail address: cyakymchuk@uwaterloo.ca (C. Yakymchuk).

68

69

70

71

72

73

74

75

76

77

78

79

80

81

82

83

84

85

86

87

88

89

90

91

92

93

94

95

96

97

98

99

100

101

102

103

104

105

106

107

108

110

111

112

113

114

115

116

117

118

119

120

121

122

123

124

125

126

127

128

129

JID:EPSL AID:118405 /SCO

2

3

6

8

10

11

12

13

14

15

16

17

18

19

20

21

22

23

24

25

26

27

28

29

30

31

32

33

34

35

36

37

38

39

40

42

43

44

45

46

47

48

49

50

51

52

53

54

55

56

57

58

59

60

61

62

63

65

C. Yakymchuk, R.M. Holder, J. Kendrick et al.

element ratios such as Sr/Y or Eu anomalies to infer the depth of melting relates to the behaviour of plagioclase and garnet, which are common reactants and products during crustal anatexis (Brown, 2013). At low pressure, plagioclase is stable during partial melting and preferentially partitions both Sr and Eu (as Eu²⁺) relative to Y and the lanthanides. Therefore, partial melt generated from a low-pressure plagioclase-bearing source has low Sr/Y and Eu/Eu* values. With increasing pressure, plagioclase becomes less stable and garnet more stable via continuous partial melting and net-transfer reactions. In mafic rocks, this change defines the facies transition from amphibolite (hornblende-plagioclase) or granulite (low-Na-pyroxene-plagioclase) to eclogite (garnet-high-Naclinopyroxene) (e.g. Moyen and Stevens, 2006). Garnet preferentially incorporates Y, reducing its availability for other phases; melt generated from a high-pressure garnet-bearing source has higher Sr/Y ratios, especially if plagioclase is absent. Garnet also preferentially incorporates Fe²⁺, relative to Fe³⁺. It has been argued that if garnet is fractionated from a rock or magma, it will increase the oxidation state of the system by removing Fe²⁺ and leaving Fe³⁺; this, in turn, will increase Eu³⁺/Eu²⁺, thereby decreasing the magnitude of Eu anomalies in zircon that subsequently grows in that system (Tang et al., 2021).

Although there is an elegance to this simple plagioclasegarnet-depth relationship, several recent studies have demonstrated that substantial differences in the Sr/Y ratio of a magma can be generated independent of depth due to the processes of melting, extraction, ascent and emplacement (Laurent et al., 2020; Kendrick and Yakymchuk, 2020) as well as the Sr/Y ratio of the starting material (Moyen, 2009). Although Sr/Y ratios of igneous rocks have been shown to correlate with crustal thickness in some modern tectonic settings and may provide a general idea of the relative behaviour of plagioclase and garnet in the source, they might not be universally robust monitors of crustal thickness (Moyen et al., 2021). This caution is particularly warranted for rocks from the Precambrian eons, when Earth's fundamental tectonic and magmatic processes might have differed (Moyen et al., 2021; Moyen and Laurent, 2018; Holder et al., 2019; Brown et al., 2020). Compared to Sr/Y whole-rock ratios, the interpretation of Eu anomalies in whole-rock samples and in zircon is further complicated by their sensitivity to oxygen fugacity (f_{02} ; Trail et al., 2012). The f₀₂ in igneous and metamorphic systems changes through the continuous nature of crystallization sequences, metamorphic reactions, and changes in other intensive system parameters such as pressure and temperature. It is also influenced by open-system processes: crystal-melt separation, devolatilization/dehydration reactions, and fluid flow. Consequently, it is unclear how sensitive Eu anomalies in zircon are to these processes and how they might influence interpretations of past crustal thickness from the zircon archive.

In this contribution, we quantitatively evaluate how Eu anomalies in zircon are expected to change during partial melting of metasedimentary rocks and metabasites at various pressuretemperature conditions (P-T) as well as during crystallization of felsic and intermediate rocks that are the primary sources of detrital zircon. We use a novel approach that combines phase equilibrium modelling, trace element partitioning, and a redox-sensitive formulation of Eu partitioning anomalies in zircon. Modelled Eu anomalies in zircon are sensitive to redox, bulk composition of the source (melting) or initial melt (crystallization), and changes in phase assemblages with temperature and pressure for the investigated rock types. Although Eu anomalies can track the complex petrological processes that operate in igneous and metamorphic systems, they are not primarily controlled by pressure. Therefore, Eu anomalies in zircon are not a simple proxy for tracking the depth of melting or crustal thickness.

2. Methods

We investigate partial melting of five rock types (three metabasic and two metasedimentary compositions) over a wide range of pressure-temperature conditions. We also model equilibrium crystallization of intermediate and felsic granitoids at mid-crustal depths (0.6 GPa). Results of the modelling are combined with trace element partitioning using lattice strain models (e.g. Blundy and Wood, 1994) when possible, and with a formulation for the Eu partitioning anomaly between melt and zircon (Trail et al., 2012) to evaluate the Eu/Eu* of zircon in equilibrium with the system as a function of pressure, temperature, mineral assemblage, and oxygen fugacity. Phase equilibrium modelling was conducted using the THERMOCALC v.3.50 software package (Powell and Holland, 1988), the Holland and Powell (2011) internally consistent database, and specifically calibrated activity-composition models for each rock type. Details are found in the Supplementary Material.

Modelled metasedimentary rocks include an average amphibolite-facies metapelite (Ague, 1991) and an average passive margin greywacke (Yakymchuk and Brown, 2014); these compositions were modelled as reported in Holder et al. (2020) using the activity-composition models of White et al. (2014). Three metabasite compositions were modelled that envelop most modern midocean ridge compositions as well as Archean basalts (supplementary Figure S3). Modelled metabasite compositions include a depleted Archean tholeiite (Condie, 1981; White et al., 2017)—which is similar in bulk composition to an average mid-ocean ridge basalt—as well as an enriched Archean tholeiite (Condie, 1981; White et al., 2017), and an Archean high-Mg basalt (Szilas et al., 2013; Kendrick and Yakymchuk, 2020). These compositions were modelled using the activity-composition models from Green et al. (2016) that were calibrated specifically for partial melting of metabasites.

Phase assemblages, proportions, and compositions as well as the chemical potential of oxygen (μO) were extracted from the THERMOCALC output for the metasedimentary rocks and metabasites across a grid with 50 °C and 0.1 GPa spacing. The concentration of H₂O for the metasedimentary compositions was used so that the melt is just saturated with H₂O at the wet solidus at 0.8 GPa; for metabasites, a just-saturated solidus with H₂O at 1.2 GPa was used. This approximates a scenario where there is only a trace amount of H₂O fluid at the onset of melting (e.g. White et al., 2007). The amounts of ferric and ferrous iron in these compositions are discussed by Yakymchuk and Brown (2014) for the metasedimentary rocks as well as Kendrick and Yakymchuk (2020) for the metabasites. Modelled compositions for each metamorphic rock are reported in Supplementary Table S1.

Crystallization of tonalite (sample 101 of Piwinskii, 1968), an average S-type granite (sample DK89 of Scaillet et al., 1995) and an A-type granite (sample GIG-1 of Clemens et al., 1986) were modelled using the activity-composition models from Holland et al. (2018) that were calibrated for crystallization of igneous rocks. We fix the crystallization pressure at 0.6 GPa, which is reasonable for emplacement in the middle crust: the results are not expected to be substantially different at pressures that reflect slightly shallower or deeper conditions as the main phase boundaries are not pressure sensitive for intermediate-felsic igneous rocks (e.g. Holland et al., 2018). For the tonalite, we model a melt with \sim 6 wt.% H_2O (Kirkland et al., 2021) with a molar $Fe^{3+}/[Fe^{2+} + Fe^{3+}]$ ratio of 0.44 (calculated from values in Piwinskii, 1968). For the S-type granite, we model a relatively dry granite (2 wt.% H₂O) with a relatively reduced $Fe^{3+}/[Fe^{2+} + Fe^{3+}]$ ratio of 0.18 (calculated from the values reported in Scaillet et al., 1995). For the A-type granite, we use an H2O concentration of 2.4 wt% (lower end of values reported in Clemens et al., 1986) and a molar $Fe^{3+}/[Fe^{2+} + Fe^{3+}]$

68

69

70

71

72

73

74 75

76

77

78

79

80

81

82

83

84

85

86

89

90

91

92

93

94

95

96

97

98

99

100

101

102

103

104

105

106

107

108

110

111

112

113

114

115

116

117

118

119

120

121

122

123

124

125

126

127

128

129

130

131

JID:EPSL AID:118405 /SCO

2

8

10

11

12

13

14

15

16

17

18

19

20

21

22

23

24

25

26

27

28

29

30

31

32

33

34

35

36

37

38

39

40

42

43

44

45

46

47

48

49

50

51

52

53

54

55

56

57

58

59

60

61

62

63

65

Earth and Planetary Science Letters ••• (••••) •••••

ratio of 0.47 (from Clemens et al., 1986). Modelled compositions for the granitoids are summarized in Supplementary Table S1.

Oxygen fugacity is an important control on Eu/Eu* of zircon (Trail et al., 2012). We report the computed oxygen fugacity relative to the nickel-nickel oxide buffer (NNO) in log units (Δ NNO). This was computed using the μ O values from the THERMOCALC output combined with the Gibbs free energy (G) values of nickel and nickel oxide from the database of Holland and Powell (2011).

The concentrations of Sm, Eu and Gd in melt-either anatectic melt in the metamorphic system or residual melt in the crystallization models-were computed using a mass balance approach with mineral/melt partition coefficients (Hanson, 1980). More details are found in the Supplementary Material.

For all minerals except zircon, we treat Eu²⁺ and Eu³⁺ separately because they partition differently into various minerals. First, we calculate the ratio of Eu^{2+}/Eu^{3+} in the system as a function of f_{O2}, temperature and melt composition using the formulation of Burnham et al. (2015); this is the same approach applied by Holder et al. (2020) to model partial melting of metasedimentary rocks. Then, separate partition coefficients are derived for Eu²⁺ and Eu³⁺ in the minerals stable at each P-T point. Mineral-melt partition coefficients and model starting concentrations are reported in Supplementary Tables S2 and S3. For most minerals, we use a lattice strain model (e.g. Blundy and Wood, 1994) to approximate the partition coefficients for Sm³⁺, Eu³⁺, Gd³⁺ and Eu²⁺ as a function of temperature as well as for pressure, mineral composition and melt compositions if these parameterizations exist. The specific models for each mineral for trivalent and divalent cations are found in Supplementary Tables S2 and S3.

For zircon, Eu/Eu* values were determined by combining the computed Eu/Eu* of the melt-based on trace element partitioning and mass balance-with the zircon/melt Eu partitioning anomaly (Eu/Eu*)_D from Trail et al. (2012). This approach is independent of using partition coefficients to model Eu concentrations in zircon; current parameterizations of zircon trace element partitioning do not separate trivalent from divalent Eu (Claiborne et al., 2018; Streicher et al., 2023) but these parameterizations are useful for modelling the other REE in zircon. In the parameterization of Trail et al. (2012), the Eu partitioning anomaly is solely a function of f_{02} and not pressure or temperature. For the metasedimentary rocks, this approach differs from that of Holder et al. (2020), who attempted to parameterize zircon Eu²⁺ and Eu³⁺ partitioning separately, as described for other phases in the previous paragraph. A more detailed explanation of the modelling and the formulations used are presented in the Supplementary Material.

Starting trace element concentrations of all modelled rock types are found in Supplementary Table S4. For simplicity, we assume that the average metapelite and average greywacke have the same bulk trace element concentrations as average post-Archean Australia shale (Taylor and McLennan, 1985). For the metamorphic systems and granitoid crystallization, we assume closed-system behaviour. The limitations of this approach are discussed later. Trace element concentrations of the model melt were determined by combining phase weight fractions (liquid and minerals) from the THERMOCALC output with the computed partition coefficients at each P-T point.

3. Results

3.1. Partial melting

Phase relations and mineral stability fields for the metamorphic rocks are summarized in Fig. 1. Results of the key variables related to zircon Eu/Eu* are shown in Fig. 2 for the metasedimentary rocks and Fig. 3 for the metabasites. This includes the proportion of plagioclase in the system-which strongly affects the Eu/Eu* of the melt—and oxygen fugacity, which influences the zircon/melt partitioning anomaly (Trail et al., 2012). For partial melting of the modelled rock types, f_{02} increases with increasing temperature, which is expected because of its dependence on T in its thermodynamic formulation (e.g. Frost, 1991). However, f_{02} relative to NNO buffer varies depending on rock type, and the mineral assemblage-both oxide and silicate minerals—that is a function of P-T conditions. For simplicity, we focus on the \triangle NNO values, which is the difference between the system f_{02} and that of the NNO buffer in log units. The Δ QFM values follow the same trends, but at slightly higher values.

3.1.1. Metasedimentary rocks

For partial melting of the metapelite and greywacke, the proportion of plagioclase decreases up temperature (Figs. 2a, e) as it is a common reactant in partial melting reactions that are strongly endothermic (e.g. Weinberg and Hasalová, 2015). Europium anomalies in the anatectic melt generated from the metapelite are positive near the solidus (Eu/Eu*>3) and decrease with increasing temperature, becoming slightly negative at ~825 °C (Fig. 2b). Melt generated from the greywacke follows a similar pattern; Eu/Eu*>2 near the solidus and becoming slightly negative at \sim 850 °C (Fig. 2f). Melt in the metapelite shows a larger change in Eu/Eu* compared with the greywacke (Fig. 2b, f). The Eu/Eu* anomalies of the melt are much more sensitive to temperature than pressure, meaning there is only a minor dependence of Eu/Eu* of the melt on depth.

The \triangle NNO values are generally flat in P-T space and roughly track the oxide assemblage, notably the growth of rutile from ilmenite-hematite breakdown at high pressures in the metapelite (Fig. 1a) and greywacke (Fig. 1b). The \triangle NNO values also show an inflection at high temperatures (~850 °C; Figs. 2c, g) that coincides with the biotite-out phase boundary (Figs. 1a, b). Therefore, fO₂ is buffered by the oxide assemblage (e.g. ilmenite, magnetite, rutile) and, to a lesser extent, the silicate mineral assemblage (e.g. biotite). Across the modelled P-T range, \triangle NNO changes by \sim 1.8 log units for the metapelite and \sim 1.6 log units for the greywacke; in general, the systems are more oxidized at higher pressures.

Zircon Eu/Eu* decreases with increasing temperature (Fig. 2d, h). Note that the Eu/Eu* values of zircon generally follow the plagioclase modal contours (Fig. 2a, e), but they are not parallel. This is because both the change in proportions of plagioclase/melt and the oxygen fugacity have resolvable influences on the zircon Eu/Eu* values during melting of metasedimentary rocks. The general trends of zircon Eu/Eu* are similar between the metapelite and greywacke, however the metapelite has higher predicted values than the greywacke at equivalent P-T conditions. For example, at 700 °C and 0.8 GPa, zircon in the metapelite is expected to have Eu/Eu* values of \sim 1.5 whereas zircon in the greywacke has values of \sim 0.8; this is due to differences in the abundance and proportions of plagioclase and melt between the metapelite and greywacke and not related to f_{02} , which is similar between the rock types at the modelled P-T conditions (Figs. 2c, g).

3.1.2. Metabasites

The behaviour of plagioclase and oxygen fugacity in the metabasites follow different trends from those of the metasedimentary rocks. Plagioclase proportions decrease with increasing pressure. At temperatures $< \sim 850-900\,^{\circ}\text{C}$, the proportion of plagioclase increases slightly with temperature as it is can be a product of amphibole-breakdown melting at low pressures (e.g. Weinberg and Hasalová, 2015). This relationship is reversed for temperatures > \sim 850–900 °C where plagioclase becomes a reactant (Fig. 3a, e, i). Modelled \triangle NNO values for the metabasites are more reduced than metasedimentary rocks at equivalent P-T conditions, although all generally increase in the metabasites with temperature except at

JID:EPSL AID:118405 /SCO

Metasedimentary rocks

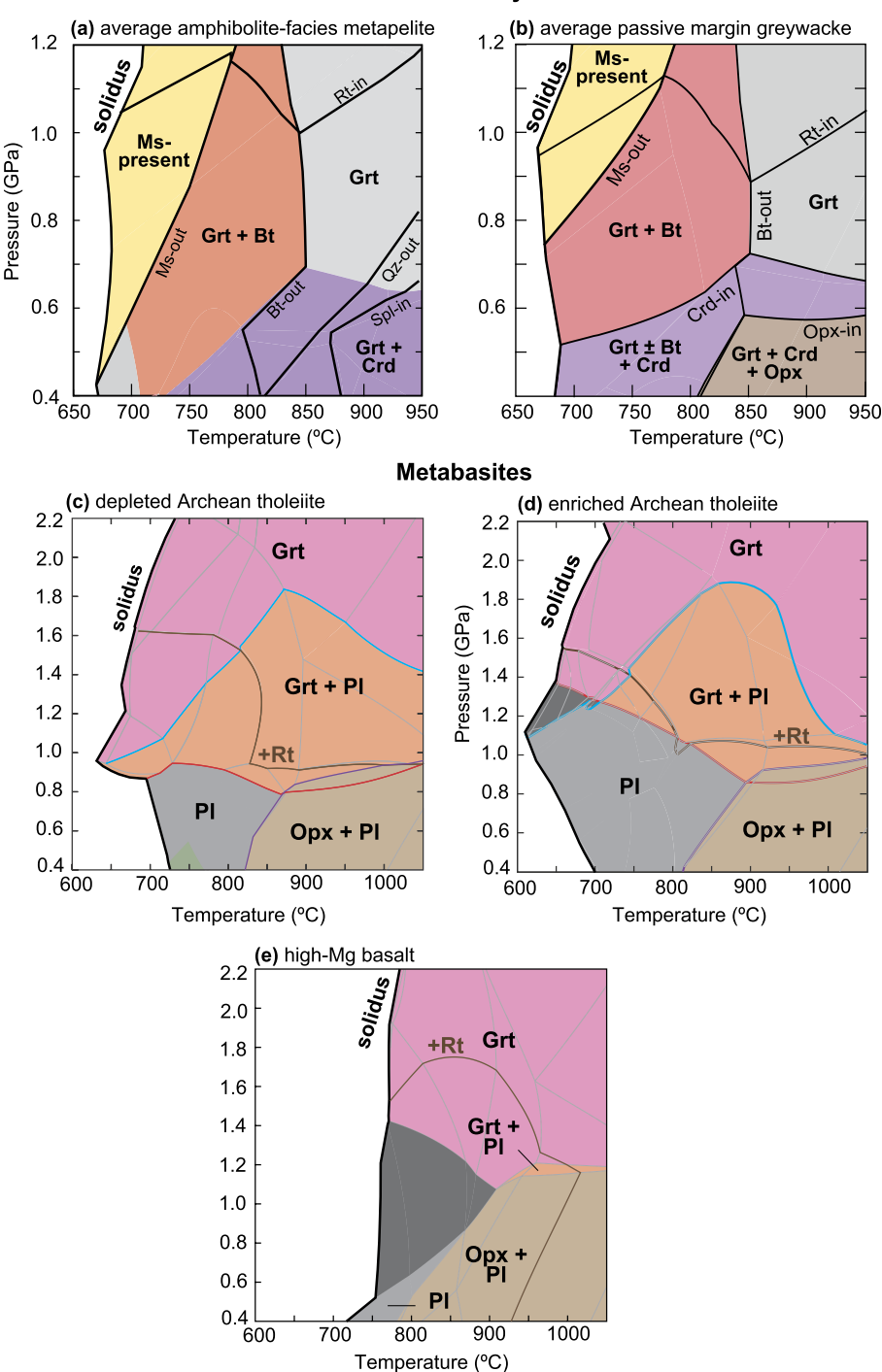


Fig. 1. Simplified pressure–temperature phase diagrams showing the stable phase assemblage for (a) an average amphibolite-facies metapelite (composition from Ague, 1991), (b) an average passive margin greywacke (composition from Yakymchuk and Brown, 2014), (c) an average depleted Archean tholeite (from Condie, 1981), (d) an average enriched Archean tholeite (from Condie, 1981), and (e) a high-Mg basalt (sample 510878 from Szilas et al., 2013). Mineral abbreviations are from Whitney and Evans (2010). The fully labelled phase diagrams are found in Yakymchuk and Brown (2014), Holder et al. (2020), and Kendrick and Yakymchuk (2020).

high-pressure granulite-facies conditions (e.g. $>800\,^{\circ}\text{C}$ and $>1.2\,$ GPa) where there are inflections that coincide with the consumption of hornblende.

Melt Eu/Eu* anomalies are highly variable with pressure and temperature. Both the depleted Archean tholeiite and enriched Archean tholeiite models have maximum Eu/Eu* melt values when epidote is present (Fig. 3b, f). In general, the metabasites have model melt Eu/Eu* that decrease with increasing temperature, and Eu/Eu* that decrease at lower pressures. The temperature-

dependence is strongest near the solidus. Contours of Eu/Eu^* in melt generally track contours of plagioclase at relatively low pressures (<1.2~GPa).

Contours of zircon Eu/Eu* are similar to those for the Eu/Eu* of melt, but with some deviation due to changes in Δ NNO with pressure and temperature. Maximum zircon Eu/Eu* values are found in the vicinity of epidote stability and the Eu/Eu* of zircon generally decrease with temperature, and mostly increase with pressure. Furthermore, the absolute values of zircon Eu/Eu* anomalies

C. Yakymchuk, R.M. Holder, J. Kendrick et al.

JID:EPSL AID:118405 /SCO

q

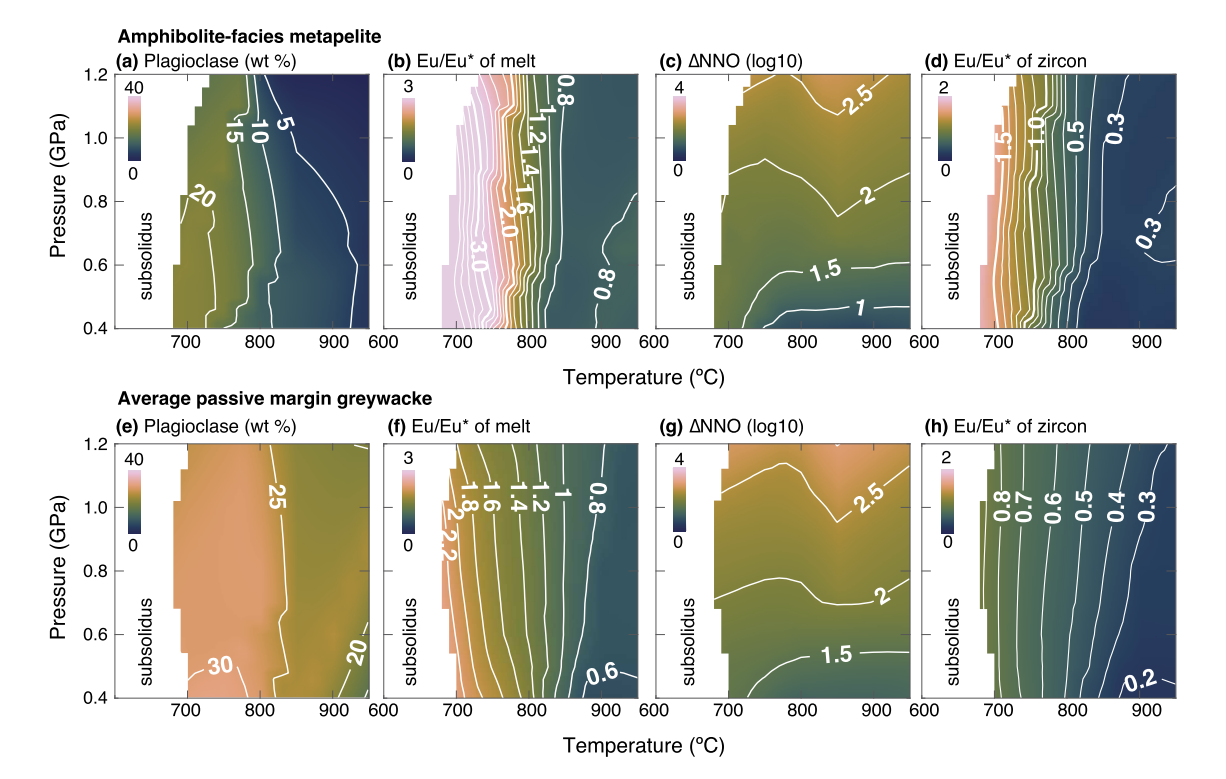


Fig. 2. Results of modelling of partial melting of metasedimentary rocks (modified from Holder et al., 2020, with zircon Eu/Eu* recalculated using the equation of Trail et al., 2012). (a, e) plagioclase proportion in the system (weight %), (b, f) Eu/Eu* (Eu_N/|Sm_N x Gd_N|^{0.5}) of the anatectic melt, (c, g) oxygen fugacity relative to the nickel-nickel oxide buffer (log units), (d, h) Eu/Eu* of zircon in equilibrium in the system. Calculated zircon Eu/Eu* anomalies are the result of both the Eu/Eu* of the melt as well as the oxygen fugacity of the system. Contours of Eu/Eu* anomalies in zircon are generally steep, which reflects the strong influence of plagioclase mode. Absolute values of zircon Eu/Eu* also vary based on the mineral assemblage as both the greywacke and metapelite were modelled with the same system concentrations of the REE.

are quite different between rock types. Consider partial melting at 1.0 GPa and 900 °C, which is generally the terminal stability of hornblende in many metabasites. Zircon from the depleted Archean tholeite has a value of \sim 0.3 (Fig. 3d), whereas the enriched Archean tholeiite has a zircon Eu/Eu* of ~0.4 (Fig. 3h), and the high-Mg basalt composition has a value of \sim 0.25 (Fig. 31).

3.2. Igneous crystallization sequences

Results for equilibrium crystallization of a model tonalite, Stype granite, and A-type granite are presented in Fig. 4.

3.2.1. Tonalite

Cooling from the tonalite liquidus (~1050°C) to the solidus (~630 °C) results in a crystallization sequence that includes plagioclase and ilmenite throughout (Fig. 4a). Hornblende is expected from >900 °C to ~700 °C; after this, biotite and minor clinopyroxene become the ferromagnesian mineral assemblage remaining during cooling to the solidus. Quartz crystallizes within 100°C of the solidus (Fig. 4a). The concentration of SiO₂ in the melt increases substantially during equilibrium crystallization (Fig. 4d). Oxygen fugacity decreases slightly from Δ NNO +4 at the liquidus to a minimum of $\triangle NNO +2$ at ~ 800 °C; this is followed by a slight increase during cooling to the solidus (Fig. 4e). The Eu/Eu* value of the melt varies from \sim 0.9 at the liquidus to \sim 0.8 near the solidus (Fig. 4f). Eu/Eu* of zircon decreases from 0.5 at the liquidus to \sim 0.35 near solidus (Fig. 4g). In general, there is a moderate change in Eu/Eu* of model zircon during crystallization of the tonalite.

3.2.2. S-type granite

The crystallization sequence of the modelled S-type granite includes plagioclase and sillimanite at high temperatures, which is followed by K-feldspar, quartz and biotite below 900 °C (Fig. 4b). Muscovite becomes stable at ~700 °C and minor ilmenite is present during the modelled crystallization sequence (Fig. 4b). The concentration of SiO₂ in the melt is stable at \sim 74 wt% during crystallization (Fig. 4d); this is due to the assemblage being quartz-buffered for most of the crystallization history. Oxygen fugacity varies from \triangle NNO of 0 at the liquidus to +2 at the solidus (Fig. 4e). The Eu/Eu* value of the melt changes from 0.4 at high temperatures to ~ 0.7 at the solidus (Fig. 4f). The modelled Eu/Eu* of zircon slightly increases from 0.15 at the liquidus to \sim 0.3 at the solidus (Fig. 4g).

3.2.3. A-type granite

The crystallization of the A-type granite is similar to that of the S-type granite (Fig. 4c) with quartz and plagioclase crystallization followed by K-feldspar at ~ 900 °C (Fig. 4c). Ilmenite is the main Fe-oxide present at high temperatures with magnetite joining the assemblage at $\sim 900\,^{\circ}$ C (Fig. 4c). Similar to the S-type granite, the SiO₂ concentration in melt is buffered by quartz for most of the crystallization sequence and stays at values of ~75 wt.% (Fig. 4d). Oxygen fugacity decreases from +3 to +1 Δ NNO at high temperatures and increases during cooling from ~800°C to the solidus (Fig. 4e). The Eu/Eu* value of the melt varies slightly from 0.3 at the liquidus to \sim 0.2 at the solidus and tracks changes in oxygen fugacity (Fig. 4e, f). Calculated Eu/Eu* in zircon decreases slightly from \sim 0.15 to \sim 0.10 during crystallization (Fig. 4g).

4. Discussion

4.1. Limitations of modelling

There are several limitations to the modelling presented here. These include: (i) the uncertainties of phase equilibrium models, (ii) variation in published partition coefficients, (iii) modelling the major minerals and not the accessory minerals for the metabasites and igneous crystallization, (iv) assuming a closed system, and (v)

C. Yakymchuk, R.M. Holder, J. Kendrick et al.

JID:EPSL AID:118405 /SCO

q



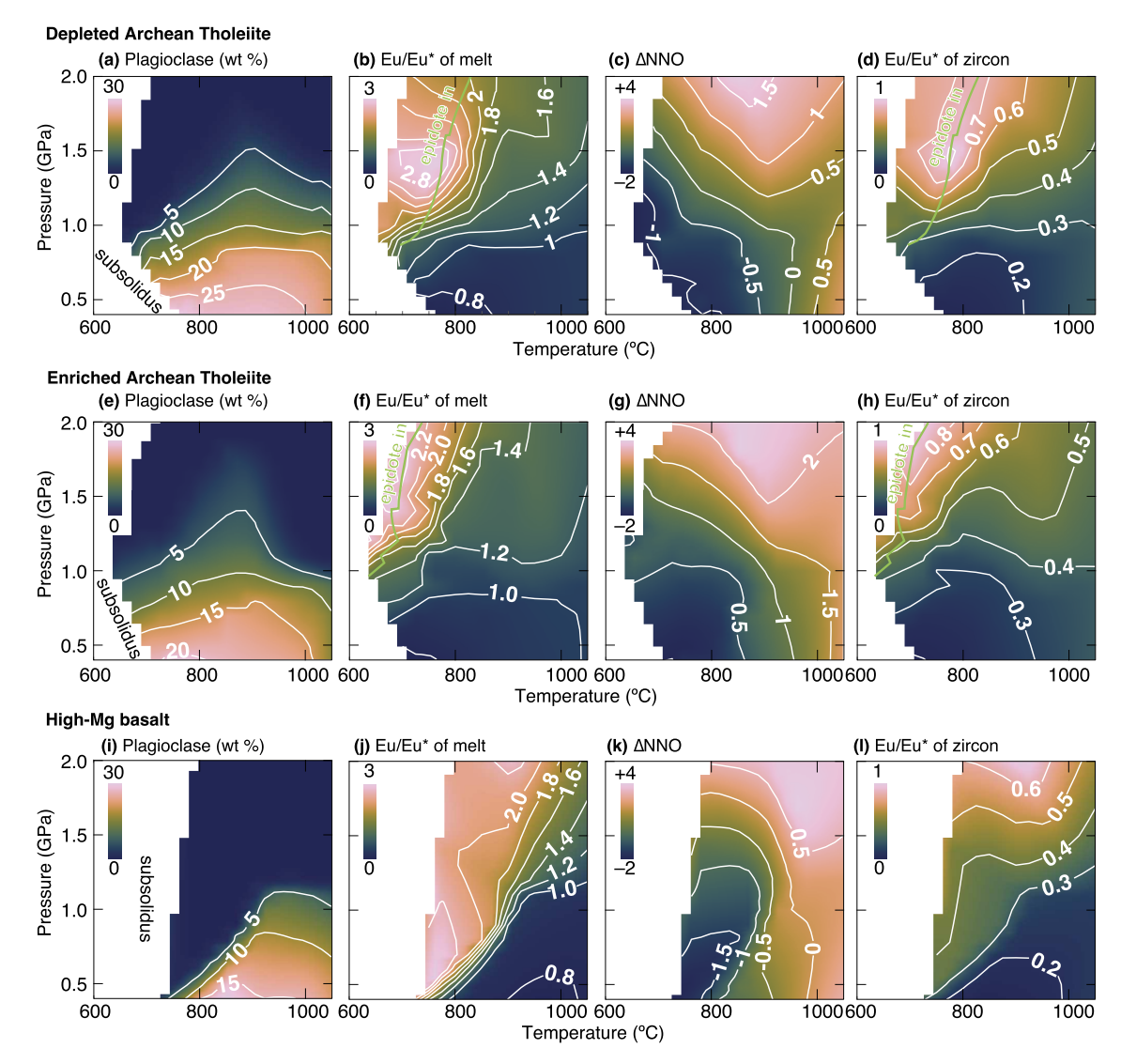


Fig. 3. Results of modelling of partial melting of metabasites. (a, e, i) plagioclase proportion in the system (weight %), (b, f, j) Eu/Eu^* ($Eu_N/[Sm_N \times Gd_N]^{0.5}$) of the anatectic melt, (c, g, k) oxygen fugacity relative to the nickel-nickel oxide buffer (log units), (d, h, l) Eu/Eu* of zircon in equilibrium in the system. Calculated zircon Eu/Eu* anomalies are the result of both the Eu/Eu* of the melt as well as the oxygen fugacity of the system. Note that contours of Eu/Eu* of zircon have generally shallow slopes in P-T space, however the absolute values are different for the various rock types.

assuming zircon is present and constantly equilibrating during the metamorphic and igneous evolutions. Uncertainties in phase equilibrium modelling are explored elsewhere (e.g. Powell and Holland, 2008) and are not repeated here. The remaining limitations in the context of modelling Eu/Eu* in zircon are considered below, but these limitations are not expected to affect the first-order results and implications of this study.

We model Eu partitioning between major minerals and melt using distribution coefficients and mass balance. When available, we use a lattice strain model for the 3+ and 2+ cations (see supplementary material). We used the mineral-melt partitioning models that are the closest match to our system and do not give unrealistic results, but many are calibrated for higher temperatures, and some require an approximation that Eu²⁺ behaves similarly to Sr²⁺, which is probably justified in most circumstances (e.g. Phillpotts, 1970). We acknowledge that different formulations of the mineral-melt distribution coefficients will yield different results. However, the general trends in the model are expected to be robust. With these limitations about our modelled distribution coefficients, our models provide first-order results that can be built upon as our understanding of the T- and f_{O2} sensitivity of REE

partitioning between minerals and melts improves with more experimental work.

Accessory minerals (zircon, monazite, and apatite) are not considered primary repositories of the investigated rare earth elements (Sm, Eu, and Gd) in our metabasite melting and granitoid crystallization models. In natural systems, the accessory minerals (monazite, apatite and allanite) can be important and even dominant repositories of the light rare earth elements (Bea, 1996; Hermann, 2002; Holder et al., 2020). Metamorphic monazite is ubiquitous in metasedimentary rocks at moderate to high temperatures (Engi, 2017). For some S-type granites, igneous monazite may be an important repository of the LREE during crystallization (Bell et al., 2019). In metabasites (and some granitoids), allanite may be present at high pressures above the solidus and may preferentially partition the LREE (Klimm et al., 2008). We note that the modelled epidote (zoisite) also strongly partitions the LREE, but the amount of allanite-zoisite in the epidote solid solution(s) will influence the results. In general, feldspars and accessory minerals compete for different Eu species. Eu²⁺ is strongly partitioned into feldspar, and this should not reflect Eu³⁺ that is taken up by zircon (Kohn and Kelly, 2018). Therefore, the absence of accessory

68

69

70

71

72

73

74

75

76

77

78

79

80

81

82

83

84

85

86

87

88

89

90

91

92

93

94

95

96

97

98

99

100

101

102

103

104

105

106

107

108

110

111

112

113

114

115

116

117

118

119

120

121

122

123

124

125

126

127

128

129

130

131

C. Yakymchuk, R.M. Holder, J. Kendrick et al.

JID:EPSL AID:118405 /SCO

2

3

5

6

8

q

10

11

12 13

14

15

16

17

18

19

20

21

22

23

24

25

26

27

28

29

30

31

32

33

34

35

36

37

38

39

40

41

42

43

44

45

46

47

48

49

50

51

52

53

54

55

56

57

58

59

60

61

62

63

64

65

66

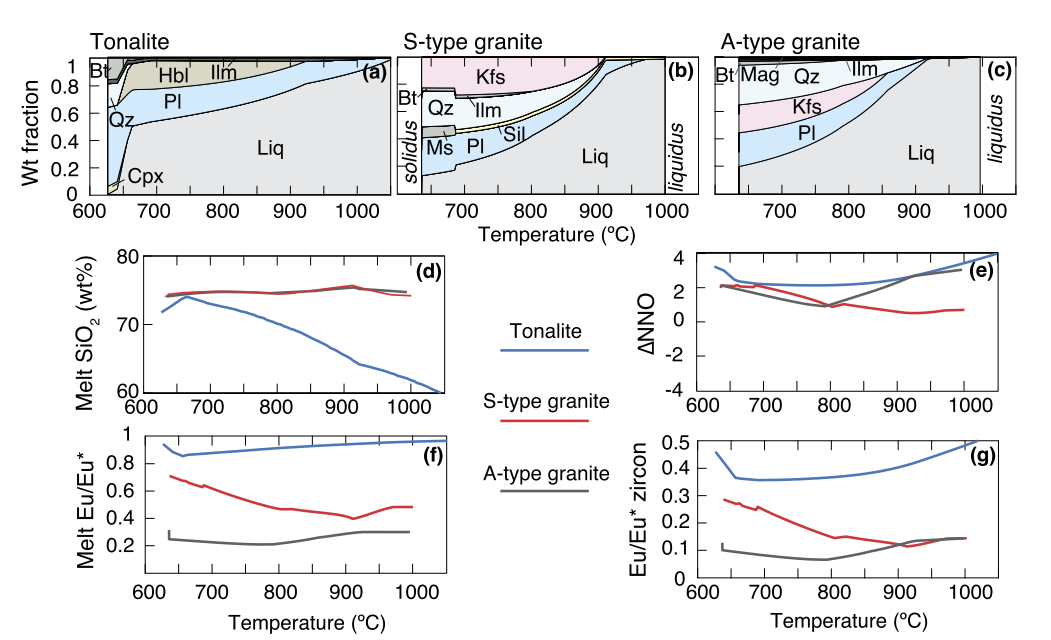


Fig. 4. Results of modelling isobaric crystallization of a tonalite, S-type granite, and A-type granite at 0.6 GPa. (a, b, c) weight fractions of phases in the system for equilibrium crystallization. (d) Concentration of SiO2 (wt%) in melt on an anhydrous basis. (e) Modelled oxygen fugacity relative to the nickel-nickel oxide buffer (log units). (f) Modelled Eu/Eu* of melt during crystallization. (g) Calculated Eu/Eu* of zircon (in equilibrium with melt) for crystallization. The Eu/Eu* of zircon varies during crystallization for all rock types. The absolute values of Eu/Eu* in zircon for the various granitoids are highly variable even though they are crystallizing at the same pressure.

minerals from our models for metabasite melting and for igneous crystallization is considered a reasonable approximation.

A final limitation of the modelling is that we consider the composition (i.e. Eu/Eu*) of zircon in equilibrium in the system over a wide range of P-T conditions; these conditions may be beyond the stability of zircon. In metamorphic systems, zircon might not be stable at ultra-high temperatures (>900 °C) due to its high solubility and grow only during cooling to the solidus (Kelsey et al., 2008). Even if zircon is present in natural samples, it is unclear if its REE composition reflects equilibrium partitioning among all phases in the system, considering the relatively slow diffusivity of the REE in minerals (e.g. Carlson, 2012) and in silicate melt (Mungall et al., 1999). In igneous systems, zircon is expected to grow when the melt becomes saturated in Zr with respect to zircon: this is a function of melt composition and temperature (Watson and Harrison, 1983) as well as the concentration of Zr in the melt. Depending on when zircon saturation is reached, zircon growth may occur during the early crystallization history or near the solidus (e.g. Harrison et al., 2007; Kirkland et al., 2021). However, zircon is expected to be a reasonable archive of the concentrations of REE in the melt from which it crystallized (Hanchar and Van Westrenen, 2007). With these limitations in mind, we now explore the implications of our modelling for interpreting Eu/Eu* values in zircon for metamorphic and igneous systems as well as for interpreting these data from detrital zircon.

4.2. Controls on Eu/Eu* in zircon

There are several important controls on the concentration of Eu-and Eu anomaly-in zircon in igneous and metamorphic systems. These include the system composition, the behaviour of the major minerals, the composition of the melt, and the redox conditions. Each of these controls is discussed below. Note that these variables are indirectly dependent on pressure and temperature. Zircon Eu/Eu* values along a series of P-T gradients are plotted against pressure (depth), plagioclase abundance, oxygen fugacity and temperature in Fig. 5.

The composition of the system (i.e. whole-rock composition) is a primary control of zircon composition. For example, metasedi-

mentary rocks commonly have negative Eu anomalies (relative to chondrite), basalt and gabbro generally have negligible Eu anomalies, and granitoids can have Eu anomalies that range from extremely negative (usually in fractionated melts; Sawyer, 1987) to extremely positive (e.g. feldspar cumulates; Kendrick et al., 2022). Zircon can grow in all of these rock types and a primary control of the Eu anomaly of newly grown zircon will be the Eu anomaly of the system in which it grows. For example, zircon associated with partial melting of metasedimentary rocks over realistic P-T gradients has modelled Eu/Eu* values that vary from 0.2 to >1 (Fig. 5a-d) whereas zircon associated with metabasite melting varies from \sim 0.2 to 0.8 (Fig. 5e-h).

All of these rock types can be metamorphosed at shallow to deep crustal (and upper mantle) conditions where various continuous reactions will consume or grow major minerals. The feldspars (plagioclase and alkali feldspar) are important repositories for Eu²⁺ and partition much less of the trivalent cations. By contrast, garnet and epidote can contain appreciable amounts of trivalent REE, but lesser amounts of Eu²⁺. In metamorphic systems, epidote is generally restricted to low-temperature melting in metabasites (i.e. at temperatures just above the wet solidus) and plagioclase may be absent or at a very minor modal proportion at these conditions (Fig. 3a, e). Anatectic melt, and zircon in equilibrium with that melt, at these conditions are expected to have higher Eu/Eu* (Fig. 3b, f).

Plagioclase behaviour varies between rock types and this impacts the relationship between P-T and the Eu/Eu* value of zircon. In metasedimentary rocks, there is a quasi-linear relationship between zircon Eu/Eu* and plagioclase abundance (Fig. 5b) and this is mainly a function of temperature and mostly independent of P-Tpath (Fig. 5d). In metabasites, plagioclase abundance is controlled mainly by pressure and not temperature; zircon Eu/Eu* anomalies in these rocks are generally independent of temperature (Fig. 5h). However, there is no systematic change of Eu/Eu* with pressure for individual P-T paths (Fig. 5e) and bulk composition also plays an important role. For example, an Eu/Eu* zircon value of 0.4 could reflect melting of a high-Mg basalt at ~30 km depth or a depleted tholeiite at \sim 50 km (Fig. 5e). Melting at a depth of \sim 60 km could yield zircon with an Eu/Eu* value of 0.45 for a high-Mg basalt or

JID:EPSL AID:118405 /SCO

Earth and Planetary Science Letters ••• (••••) •••••

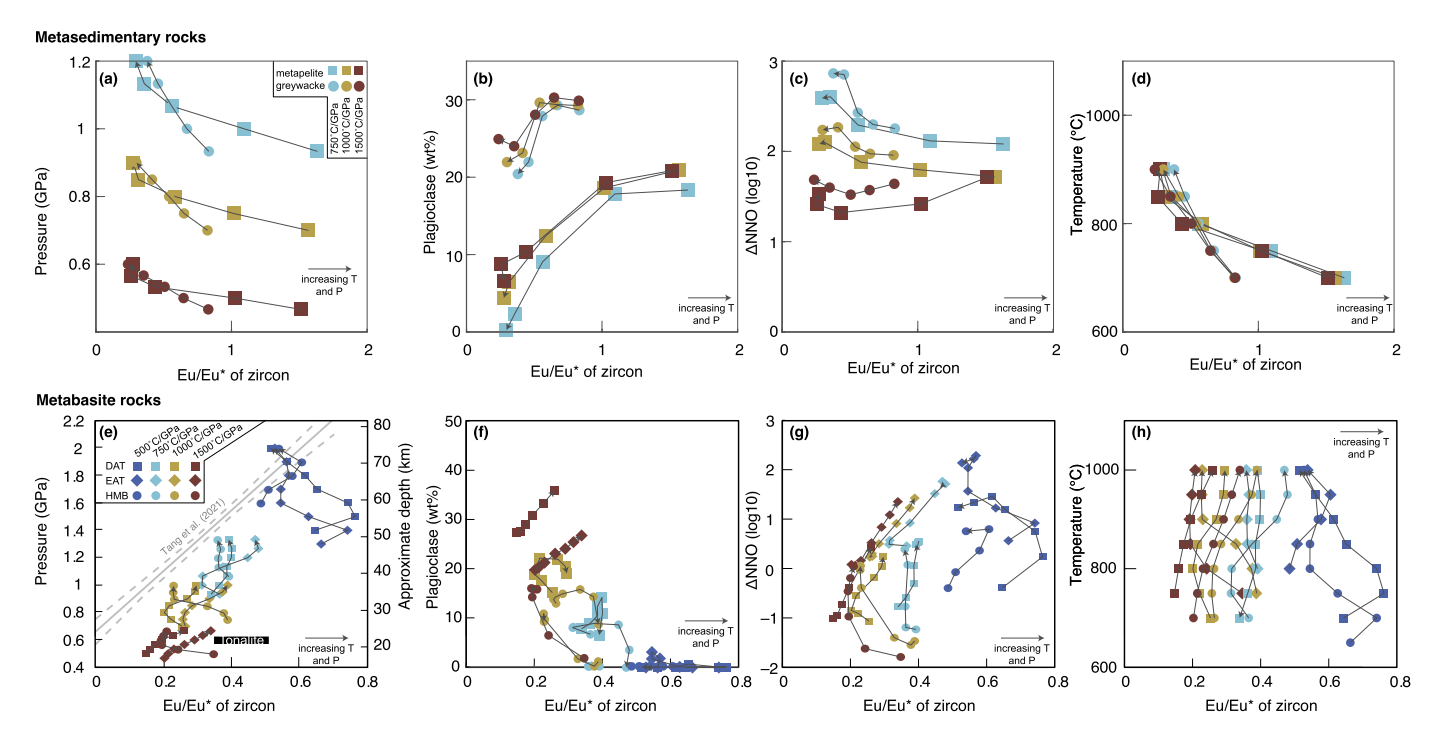


Fig. 5. Summary of modelling results. (a, e) Pressure of melting versus Eu/Eu* of zircon. Also plotted in (e) is the zircon barometer of Tang et al. (2021) that relates crustal depth to Eu/Eu* in zircon. The range of Eu/Eu* values predicted for zircon from tonalite is shown as a horizontal bar in (e). (b, f) Weight percentage of plagioclase in the residue versus Eu/Eu* of zircon. (c, g) Oxygen fugacity relative to the Nickel-Nickel-oxide (NNO) buffer versus Eu/Eu* of zircon. (d, h) Temperature versus Eu/Eu* of zircon. Results are plotted every 50 °C for apparent thermal gradients of 500, 750, 1000, and 1500 °C/GPa that bracket most metamorphic conditions throughout Earth's history (Brown et al., 2020). Black lines track the apparent thermal gradient up temperature and pressure. No results for the metasedimentary rocks were plotted for the 500 °C/GPa gradient as these were outside the modelled P-T range for these rock types.

0.75 for a depleted tholeiite (Fig. 5e). Eu/Eu* values of zircon also do not decrease systematically with increasing depth for individual P-T paths. Consider high-pressure-low-temperature metamorphism (500 °C/GPa) of an enriched Archean tholeiite (Fig. 5e). This P-T path results in a decrease in zircon Eu/Eu* with *increasing* pressure (Fig. 5e), which is opposite to the general model of increasing zircon Eu/Eu* with pressure for melt derived from mafic rocks (e.g. Tang et al., 2021).

Europium anomalies in zircon and other accessory minerals (e.g. monazite) have been used as a proxy to understand the timing of zircon growth relative to the growth or breakdown of plagioclase in metamorphic and igneous systems (Rubatto, 2017). The rationale is that europium will preferentially partition into plagioclase and alkali feldspar and this should be reflected by a decreased concentration of Eu relative to Sm and Gd in zircon that is growing in the presence of abundant plagioclase. However, this relies on the assumption that divalent europium (Eu²⁺) is an important species in the system; trivalent europium (Eu³⁺) should behave like Sm³⁺ and Gd³⁺. Therefore, the proportion of trivalent versus divalent Eu in a system is an important consideration. If all Eu in a rock were Eu³⁺, Eu/Eu* of minerals should be invariant and match the whole-rock Eu/Eu* value.

The proportion of Eu^{2+} to Eu^{3+} in silicate melt is a function of temperature, f_{02} , and melt composition (Burnham et al., 2015). Holder et al. (2020) explored the controls on the proportion of Eu^{3+} in silicate melt during partial melting of metasedimentary rocks, so we focus here on the controls during partial melting of metabasites. We note that our modelled zircon Eu/Eu^* in equilibrium with metasedimentary melt is different than theirs due to differences in the approach used. Holder et al. (2020) assumed negligible Eu^{2+} incorporation into zircon such that contours of zircon Eu/Eu^* essentially parallelled Eu^{3+}/Eu^{2+} and Δ NNO of the system. That approach was limited by a lack of data on separate partitioning of Eu^{2+} and Eu^{3+} into zircon. We used the experimen-

tal zircon:melt Eu/Eu* partitioning equation of Trail et al. (2012); this also depends on ΔNNO , but incorporation of Eu²+ and Eu³+ into zircon is implicitly tied to a much-better understood incorporation of Eu²+ and Eu³+ into melt. For this reason, for specific cases of zircon partitioning in metasedimentary rocks, we favour the present models.

The proportion of Eu³⁺ generally increases with pressure and with temperature during partial melting of metabasites (Supplementary Figure S2). At granulite-facies and high-P granulite facies conditions, more than half of Eu is expected to be trivalent for the depleted Archean tholeiite and enriched Archean tholeiite compositions. This reduces the effect of plagioclase fractionation of Eu²⁺ at these conditions because less of the Eu is divalent than at lower pressures. The role of other minerals becomes increasingly important for partitioning Eu, which is mostly trivalent under these conditions. Therefore, there is not a simple linear relationship between plagioclase abundance and Eu/Eu* anomalies in zircon, especially at moderate to high pressures during partial melting of metabasites.

Another consideration of using Eu anomalies in zircon to infer the depths of source melting (Tang et al., 2021) or secular change in geodynamic processes (e.g. Triantafyllou et al., 2022) is that the simple crystallization of granitoids can cause variable Eu/Eu* in the melt and zircon. Fractional crystallization will amplify this effect; fractional crystallization of plagioclase will change the Eu²⁺/Eu³⁺ of the system and fractionation of ilmenite (or other oxide) can change the Fe²⁺/Fe³⁺ and f_{02} values of the system. Zircon Eu/Eu* values will be a function of the Eu/Eu* of the melt when zircon is growing. Granitoids can record Ti-in-zircon temperatures from the wet-solidus (e.g. Kirkland et al., 2021; Laurent et al., 2022) to >900 °C (e.g. Moecher et al., 2014). Most granitoids have zircon that yield Ti-in-zircon temperatures of 650–850 °C over Earth's history (Balica et al., 2020). Considering the uncertainties in titania activity during melt crystallization—especially in the detrital

68

69 70

71

72

73

74

75 76

77

78

79

80

81

82

83

84

85

86

87

88

89

90

91

92

93

94

95

96

97

98

99

100

101

102

103

104

105

106

107

108

109

110

111

112

113

114

115

116

117

118

119

120

121

122

123

124

125

126

127

128

129

130

131

C. Yakymchuk, R.M. Holder, J. Kendrick et al.

JID:EPSL AID:118405 /SCO

2

3

5

6

7

8

q

10

11

12 13

14

15

16

17

18

19

20

21

22

23

24

25

26

27

28

29

30

31

32

33

34

35

36

37

38

39

40

41

42

43

44

45

46

47

48

49

50

51

52

53

54

55

56

57

58

59

60

61

62

63

64

65

66

Earth and Planetary Science Letters ••• (••••) •••••

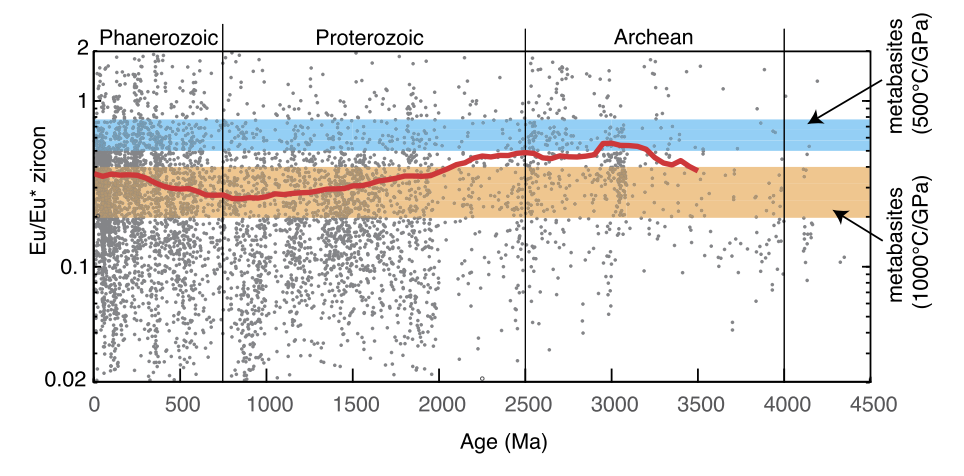


Fig. 6. Zircon Eu/Eu* through time (grey dots; data from Triantafyllou et al., 2022). The moving mean (red line) represents 50 Myr moving window averaged every 5 Myr. The average was stopped at 3500 Ma due to the paucity of data from the early Archean. The range of modelled zircon Eu/Eu* values associated with equilibrium partial melting of metabasites at are plotted for two thermal gradients that encompass most apparent thermal gradients from the Precambrian (Holder et al., 2019). The decrease in the average Eu/Eu* of zircon from the Archean to the Proterozoic could reflect a changing thermal regime or, alternatively, an increase in reworking of supracrustal material in the deep crust.

zircon record-the temperatures may have been even higher (e.g. Schiller and Finger, 2019). The modelled tonalite shows a zircon Eu/Eu* value that varies from \sim 0.35 to \sim 0.45 at temperatures between 700 °C and the wet solidus; this is when most zircon is expected to crystallize (e.g. Kirkland et al., 2021). Changes in Eu/Eu* in zircon during crystallization are documented in plutons and reflect plagioclase crystallization and fractionation (e.g. Schaen et al., 2017). However, the values and ranges of Eu/Eu* in magmatic zircon suites will also be sensitive to the P-T conditions, mineral assemblages, f_{02} , and starting composition of the metabasite source (see Fig. 3).

In summary, there is no simple relationship between depth and Eu/Eu* in zircon. Although there is some correlation between zircon Eu/Eu* and pressure (depth) for metabasite melting, other variables-temperature, melt fraction, source rock composition, and f_{O2}—also significantly influence Eu/Eu* in zircon during anatexis of metabasites and metasedimentary rocks (Figs. 2, 3) as well as during granitoid crystallization (Fig. 4).

4.3. Potential applications of Eu/Eu* anomalies in zircon

Considering the various processes that influence Eu/Eu* in zircon during partial melting and melt crystallization, there is not expected to be a simple relationship between Eu/Eu* in zircon with depth. There is a minor correlation between plagioclase modes and zircon Eu/Eu* (Figs. 5b, f), but this relationship is complicated by changing f_{02} during partial melting. This is reflected by the increasing importance of the other major minerals that prefer trivalent Eu. Considering the limitations we have discussed here, there are several opportunities for using Eu/Eu* in zircon to understand the petrogenesis of granitoids and the geodynamic mechanisms that generate them.

Europium anomalies in zircon are predicted to change with progressive crystallization of feldspar in granitoids (Fig. 4). Linking zircon Eu/Eu* from variably fractionated granitoid suites can be used to understand feldspar behaviour during the evolution of crystal mushes and explore the factors that contribute to rhyolite volcanism (Schaen et al., 2017). Interrogating intercrystal and intracrystal variations in zircon Eu/Eu* values and U-Pb dates may also elucidate the role of open- and closed-system processes during and after the generation and crystallization of granitoids.

Oxygen fugacity is a key factor that controls redox-sensitive elements during partial melting and granitoid petrogenesis. If the f_{02} of melt can be independently constrained, this could allow us to control for this factor in Eu/Eu* anomalies in zircon and allow us to interrogate Eu anomalies in zircon to understand the depths and temperatures of partial melting and melt crystallization. Considering that Ce is also redox sensitive (e.g. Trail et al., 2012), pairing Eu and Ce anomalies in zircon can be used to model f_{02} changes and better evaluate the residual mineral assemblages during partial melting and the crystallization sequences during magma cooling. Loader et al. (2022) modelled Ce anomalies in zircon to calculate the temperatures and nature of the co-crystallizing phases in a Cu porphyry system. Such applications are an important prospect for linking the zircon composition to mineralization systems.

If we can rule out source depth as a primary cause of Eu/Eu* variations in zircon, this opens up other hypotheses to explain secular change in zircon Eu/Eu* over time. Triantafyllou et al. (2022) document a decrease in zircon Eu/Eu* from the Archean to the Proterozoic (Fig. 6) that was interpreted to represent a change in geodynamic environments. If partial melting or fractional crystallization of metabasites was the dominant cause of continent (and zircon) growth, then this change could reflect a change in the apparent thermal gradients of metamorphism/fractionation in the deep crust (Fig. 6). An alternative explanation is that sources of detrital zircon evolved from predominately juvenile TTG suites with higher zircon Eu/Eu* values (e.g. 0.3-0.5 in Fig. 3) to zircon generated from partial melting of metasedimentary rocks with lower zircon Eu/Eu* values that are increasingly more reduced (e.g. due to the presence of organic material). Although our modelled metasedimentary compositions yield zircon Eu/Eu* values similar to those from the metabasites, more reduced metasedimentary rocks-that are quite common (Forshaw and Pattison, 2023)-are expected to yield even lower zircon Eu/Eu* values. This is apparent from the strongly negative Eu anomalies in S-type granites (e.g. Villaros et al., 2009). Therefore, an increase in the input of relatively reduced sedimentary material into the deep crust could decrease the Eu/Eu* values of zircon through time. The increased importance of recycled surface-derived material to the magmatic zircon record is apparent from the increase in δ^{18} O values of magmatic zircon over time (e.g. Valley et al., 2005).

Utilizing detrital zircon Eu/Eu* anomalies is a potentially important archive of secular change on Earth. We caution against inferring simple relationships between zircon Eu/Eu* and depth or plagioclase proportions considering the variety of factors that contribute to zircon trace element compositions. However, careful integration of Eu/Eu* in zircon with other data has the potential to reveal new insights into Earth's evolution.

68

69

70

71

72

73

74

75

76

77

78

79

80

81

82

83

84

85

86

87

88

89

90

91

92

93

94

95

96

97

98

99

100

101

102

103

104

105

106

107

108

109

110

111

112

113

114

115

116

117

118

119

120

121

122

123

124

125

126

127

128

129

130

131

C. Yakymchuk, R.M. Holder, J. Kendrick et al.

Earth and Planetary Science Letters ••• (•••) •••••

5. Conclusions

2

3

10

11

12

13

14

15

16

17

18

19

20

21

22

23

24

25

26

27

28

29

30

31

32

33

34

35

36

37

38

39

40

41

42

43

45

46

47

48

49

50

51

52

53

54

55

56

57

58

59

60

61

62

63

65

66

JID:EPSL AID:118405 /SCO

We investigate the controls on Eu anomalies in zircon using phase equilibrium modelling of partial melting of metasedimentary rocks and metabasites as well as felsic and intermediate magma crystallization. Europium anomalies in melt in anatectic systems are controlled by the bulk rock composition, the phase assemblage (including plagioclase and the other minerals), and oxygen fugacity. There is an interplay between the changing oxidation state of Eu and the role of the minerals that preferentially partition trivalent Eu. There are no systematic changes in zircon Eu/Eu* with pressure and temperature that are applicable to all the investigated rock types. Isobaric crystallization of granitoids results in a wide range of Eu/Eu* anomalies in zircon that reflects changing oxygen fugacity and the crystallization sequence. Considering the variety of rock types that contribute to the detrital zircon record and the extreme variability of Eu/Eu* ratios in the small subset of rock types that we have investigated, we suggest that Eu anomalies in zircon are not an appropriate proxy for crustal depth but do provide a monitor of the complex petrogenesis of granitoids from source to sink.

CRediT authorship contribution statement

Chris Yakymchuk: Writing – review & editing, Writing – original draft, Visualization, Validation, Methodology, Investigation, Formal analysis, Data curation, Conceptualization. **Robert M. Holder:** Writing – review & editing, Methodology, Investigation. **Jillian Kendrick:** Writing – review & editing, Methodology, Investigation, Data curation. **Jean-François Moyen:** Writing – review & editing, Methodology, Conceptualization.

Declaration of competing interest

The authors declare that they have no known competing financial interests or personal relationships that could have appeared to influence the work reported in this paper.

Data availability

Data will be made available on request.

Acknowledgements

We thank F. Finger and C. Balica for constructive reviews and R. Hickey-Vargas for editorial handling.

Funding: Yakymchuk acknowledges funding from the Natural Sciences and Engineering Research Council of Canada. Holder acknowledges funding from the United States National Science Foundation, EAR 2022746.

Appendix A. Supplementary material

Supplementary material related to this article can be found online at https://doi.org/10.1016/j.epsl.2023.118405.

References

- Ague, J.J., 1991. Evidence for major mass transfer and volume strain during regional metamorphism of pelites. Geology 19, 855–858.
- Balica, C., Ducea, M.N., Gehrels, G.E., Kirk, J., Roban, R.D., Luffi, P., Chapman, J.B., Triantafyllou, A., Guo, J., Stoica, A.M., 2020. A zircon petrochronologic view on granitoids and continental evolution. Earth Planet. Sci. Lett. 531, 116005.
- Ballard, J.R., Palin, M.J., Campbell, I.H., 2002. Relative oxidation states of magmas inferred from Ce (IV)/Ce (III) in zircon: application to porphyry copper deposits of northern Chile. Contrib. Mineral. Petrol. 144, 347–364.
- Bea, F., 1996. Residence of REE, Y, Th and U in granites and crustal protoliths; implications for the chemistry of crustal melts. J. Petrol. 37, 521–552.

- Bell, E.A., Boehnke, P., Barboni, M., Harrison, T.M., 2019. Tracking chemical alteration in magmatic zircon using rare Earth element abundances. Chem. Geol. 510, 56–71.
- Blundy, J., Wood, B., 1994. Prediction of crystal-melt partition coefficients from elastic moduli. Nature 372, 452–454.
- Brown, M., 2013. Granite: from genesis to emplacement. Geol. Soc. Am. Bull. 125, 1079–1113.
- Brown, M., Johnson, T., Gardiner, N.J., 2020. Plate tectonics and the Archean Earth. Annu. Rev. Earth Planet. Sci. 48, 291–320.
- Burnham, A.D., Berry, A.J., Halse, H.R., Schofield, P.F., Cibin, G., Mosselmans, J., 2015. The oxidation state of europium in silicate melts as a function of oxygen fugacity, composition and temperature. Chem. Geol. 411, 248–259.
- Carlson, W.D., 2012. Rates and mechanism of Y, REE, and Cr diffusion in garnet. Am. Mineral. 97, 1598–1618.
- Chapman, J.B., Ducea, M.N., DeCelles, P.G., Profeta, L., 2015. Tracking changes in crustal thickness during orogenic evolution with Sr/Y: an example from the North American Cordillera. Geology 43, 919–922.
- Claiborne, L.L., Miller, C.F., Gualda, G.A., Carley, T.L., Covey, A.K., Wooden, J.L., Fleming, M.A., 2018. Zircon as magma monitor: robust, temperature-dependent partition coefficients from glass and zircon surface and rim measurements from natural systems. In: Moser, D., Corfu, F., Darling, J.R., reddy, S.M., Tait, K. (Eds.), Microstructural Geochronology: Planetary Records Down to Atom Scale. In: Geophysical Monograph Series, vol. 232. AGU Books, Washington DC, USA, pp. 1–33.
- Clemens, J.D., Holloway, J.R., White, A., 1986. Origin of an A-type granite; experimental constraints. Am. Mineral. 71, 317–324.
- Condie, K.C., 1981. Archean Greenstone Belts. Developments in Precambrian Geology, vol. 3. Elsevier, New York.
- Engi, M., 2017. Petrochronology based on REE-minerals: monazite, allanite, xenotime, apatite. Rev. Mineral. Geochem. 83, 365–418.
- Forshaw, J.B., Pattison, D.R., 2023. Major-element geochemistry of pelites. Geology 51, 39-43.
- Frost, B.R., 1991. Introduction to oxygen fugacity and its petrologic importance. In: Lindsley, D.H. (Ed.), Oxide Minerals: Petrologic and Magnetic Significance. In: Reviews in Mineralogy, vol. 25, pp. 1–8.
- Green, E., White, R.W., Diener, J., Powell, R., Holland, T., Palin, R.M., 2016. Activity-composition relations for the calculation of partial melting equilibria in metabasic rocks. J. Metamorph. Geol. 34, 845–869.
- Hanchar, J.M., Van Westrenen, W., 2007. Rare Earth element behavior in zircon-melt systems. Elements 3, 37–42.
- Hanson, G.N., 1980. Rare Earth elements in petrogenetic studies of igneous systems.

 Annu. Rev. Earth Planet. Sci. 8, 371–406.
- Harrison, T.M., Watson, E.B., Aikman, A.B., 2007. Temperature spectra of zircon crystallization in plutonic rocks. Geology 35, 635–638.
- Hermann, J., 2002. Allanite: thorium and light rare Earth element carrier in subducted crust. Chem. Geol. 192, 289–306.
- Hinton, R.W., Upton, B., 1991. The chemistry of zircon: variations within and between large crystals from syenite and alkali basalt xenoliths. Geochim. Cosmochim. Acta 55, 3287–3302.
- Holder, R.M., Viete, D.R., Brown, M., Johnson, T.E., 2019. Metamorphism and the evolution of plate tectonics. Nature 572, 378–381.
- Holder, R.M., Yakymchuk, C., Viete, D.R., 2020. Accessory mineral Eu anomalies in suprasolidus rocks: beyond feldspar. Geochem. Geophys. Geosyst. 21, e2020GC009052.
- Holland, T.J.B., Green, E.C.R., Powell, R., 2018. Melting of peridotites through to granites: a simple thermodynamic model in the system KNCFMASHTOCr. J. Petrol. 59, 881–900.
- Holland, T., Powell, R., 2011. An improved and extended internally consistent thermodynamic dataset for phases of petrological interest, involving a new equation of state for solids. J. Metamorph. Geol. 29, 333–383.
- Kelsey, D.E., Clark, C., Hand, M., 2008. Thermobarometric modelling of zircon and monazite growth in melt-bearing systems: examples using model metapelitic and metapsammitic granulites. J. Metamorph. Geol. 26, 199–212.
- Kendrick, J., Duguet, M., Yakymchuk, C., 2022. Diversification of Archean tonalite-trondhjemite-granodiorite suites in a mushy middle crust. Geology 50, 76–80.
- Kendrick, J., Yakymchuk, C., 2020. Garnet fractionation, progressive melt loss and bulk composition variations in anatectic metabasites: complications for interpreting the geodynamic significance of TTGs. Geosci. Front. 11, 745–763.
- Kirkland, C.L., Yakymchuk, C., Olierook, H.K.H., Hartnady, M.I.H., Gardiner, N.J., Moyen, J., Smithies, R.H., Szilas, K., Johnson, T.E., 2021. Theoretical versus empirical secular change in zircon composition. Earth Planet. Sci. Lett. 554, 116660.
- Klimm, K., Blundy, J.D., Green, T.H., 2008. Trace element partitioning and accessory phase saturation during H2O-saturated melting of basalt with implications for subduction zone chemical fluxes. J. Petrol. 49, 523–553.
- Kohn, M.J., Kelly, N.M., 2018. Petrology and geochronology of metamorphic zircon. In: Moser, D., Corfu, F., Darling, J.R., reddy, S.M., Tait, K. (Eds.), Microstructural Geochronology: Planetary Records down to Atom Scale. In: Geophysical Monograph Series, vol. 232. AGU Books, Washington DC, USA, pp. 35–61.
- Laurent, O., Björnsen, J., Wotzlaw, J.F., Bretscher, S., Pimenta Silva, M., Moyen, J.F., Ulmer, P., Bachmann, O., 2020. Earth's earliest granitoids are crystal-rich magma reservoirs tapped by silicic eruptions. Nat. Geosci. 13, 163–169.

68

69

70

71

72

73

74

75

76

77

78

79

80

81

82

83

84

85

86

87

88

89

90

91

92

93

94

95

96

97

98

99

100

101

102

103

104

105

113 114

115

116

117

118

119

120

121

122

123

124 125

126

127

128

129 130

131

132

JID:EPSL AID:118405 /SCO

2

3

5

6

7

8

q

10

11

12

13

14

15

16

17

18

19

20

21

22

23

24

25

26

27

28

29

30

31

32

33

34

35

36

37

38

39

40

47

49

50

51

52

53

54

55

56

57

58

59 60

61

62

63

65

66

- Laurent, O., Moyen, J., Wotzlaw, J., Björnsen, J., Bachmann, O., 2022. Early Earth
- zircons formed in residual granitic melts produced by tonalite differentiation. Geology 50, 437-441.
- Loader, M.A., Nathwani, C.L., Wilkinson, J.J., Armstrong, R.N., 2022. Controls on the magnitude of Ce anomalies in zircon, Geochim, Cosmochim, Acta 328, 242-257.
- Moecher, D.P., McDowell, S.M., Samson, S.D., Miller, C.F., 2014. Ti-in-zircon thermometry and crystallization modeling support hot Grenville granite hypothesis. Geology 42, 267-270.
- Moyen, J.F., 2009. High Sr/Y and La/Yb ratios: the meaning of the "adakitic signature" Lithos 112 556-574
- Moyen, J.F., Stevens, G., 2006. Experimental Constraints on TTG Petrogenesis: Implications for Archean Geodynamics. Geophysical Monograph, vol. 164. American Geophysical Union, pp. 149–175.
- Moyen, J.F., Laurent, O., 2018. Archaean tectonic systems: a view from igneous rocks. Lithos 302, 99-125.
- Moyen, J., Janoušek, V., Laurent, O., Bachmann, O., Jacob, J., Farina, F., Fiannacca, P., Villaros, A., 2021. Crustal melting vs. fractionation of basaltic magmas: part 1, granites and paradigms, Lithos 402, 106291.
- Mungall, J.E., Dingwell, D.B., Chaussidon, M., 1999. Chemical diffusivities of 18 trace elements in granitoid melts. Geochim. Cosmochim. Acta 63, 2599-2610.
- Murali, A.V., Parthasarathy, R., Mahadevan, T.M., Das, M.S., 1983. Trace element characteristics, REE patterns and partition coefficients of zircons from different geological environments-a case study on Indian zircons. Geochim. Cosmochim. Acta 47, 2047-2052.
- Philpotts, J.A., 1970. Redox estimation from a calculation of Eu2+ and Eu3+ concentrations in natural phases, Earth Planet, Sci. Lett. 9, 257-268.
- Piwinskii, A.J., 1968. Experimental studies of igneous rock series central Sierra Nevada batholith, California. J. Geol. 76, 548-570.
- Powell, R., Holland, T., 2008. On thermobarometry. J. Metamorph. Geol. 26, 155-179. Powell, R., Holland, T., 1988. An internally consistent dataset with uncertainties and correlations: 3. Applications to geobarometry, worked examples and a computer program. J. Metamorph. Geol. 6, 173-204.
- Rubatto, D., 2002. Zircon trace element geochemistry: partitioning with garnet and the link between U-Pb ages and metamorphism. Chem. Geol. 184, 123-138.
- Rubatto, D., 2017. Zircon: the metamorphic mineral. Rev. Mineral. Geochem. 83, 261-295
- Rudnick, R.L., 1992. Restites, Eu anomalies and the lower continental crust. Geochim. Cosmochim. Acta 56, 963-970.
- Sawyer, E.W., 1987. The role of partial melting and fractional crystallization in determining discordant migmatite leucosome compositions. J. Petrol. 28, 445-473.
- Scaillet, B., Pichavant, M., Roux, J., 1995. Experimental crystallization of leucogranite magmas. J. Petrol. 36, 663-705.
- Schaen, A.J., Cottle, J.M., Singer, B.S., Keller, C.B., Garibaldi, N., Schoene, B., 2017. Complementary crystal accumulation and rhyolite melt segregation in a late Miocene Andean pluton. Geology 45, 835-838.

- Schiller, D., Finger, F., 2019. Application of Ti-in-zircon thermometry to granite studies: problems and possible solutions. Contrib. Mineral. Petrol. 174, 1-16.
- Streicher, L.B., van Westrenen, W., Hanchar, J.M., Brouwer, F.M., 2023. A REE-based zircon geothermometer based on improved lattice strain modeling of zirconmelt REE partition coefficients, Geochim, Cosmochim, Acta 346, 54-64.
- Szilas, K., Van Hinsberg, V.J., Kisters, A.F.M., Hoffmann, J.E., Windley, B.F., Kokfelt, T.F., Scherstén, A., Frei, R., Rosing, M.T., Muenker, C., 2013. Remnants of arc-related Mesoarchaean oceanic crust in the Tartoq Group of SW Greenland. Gondwana Res 23 436-451
- Tang, M., Ji, W., Chu, X., Wu, A., Chen, C., 2021. Reconstructing crustal thickness evolution from europium anomalies in detrital zircons. Geology 49, 76-80.
- Taylor, S.R., McLennan, S.M., 1985. The Continental Crust: Its Composition and Evolution, Blackwell, Oxford, UK.
- Trail, D., Watson, E.B., Tailby, N.D., 2012. Ce and Eu anomalies in zircon as proxies for the oxidation state of magmas. Geochim. Cosmochim. Acta 97, 70-87.
- Triantafyllou, A., Ducea, M.N., Jepson, G., Hernández-Montenegro, J.D., Bisch, A., Ganne, J., 2022. Europium anomalies in detrital zircons record major transitions in Earth geodynamics at 2.5 Ga and 0.9 Ga. Geology. https://doi.org/10.1130/ G50720 1
- Valley, J.W., Lackey, J.S., Cavosie, A.J., Clechenko, C.C., Spicuzza, M.J., Basei, M.A.S., Bindeman, I.N., Ferreira, V.P., Sial, A.N., King, E.M., 2005. 4.4 billion years of crustal maturation: oxygen isotope ratios of magmatic zircon. Contrib. Mineral. Petrol. 150, 561-580.
- Villaros, A., Stevens, G., Moyen, J.F., Buick, I.S., 2009. The trace element compositions of S-type granites: evidence for disequilibrium melting and accessory phase entrainment in the source, Contrib. Mineral, Petrol, 158, 543-561.
- Watson, E.B., Harrison, T.M., 1983. Zircon saturation revisited: temperature and composition effects in a variety of crustal magma types. Earth Planet. Sci. Lett. 64, 295-304.
- Weill, D.F., Drake, M.J., 1973. Europium anomaly in plagioclase feldspar: experimental results and semiguantitative model. Science 180, 1059-1060.
- Weinberg, R.F., Hasalová, P., 2015. Water-fluxed melting of the continental crust: a review. Lithos 212, 158-188.
- White, R.W., Powell, R., Holland, T., 2007. Progress relating to calculation of partial melting equilibria for metapelites. J. Metamorph. Geol. 25, 511-527.
- White, R.W., Powell, R., Johnson, T.E., 2014. The effect of Mn on mineral stability in metapelites revisited: new a-x relations for manganese-bearing minerals. J. Metamorph. Geol. 32, 809-828.
- White, R.W., Palin, R.M., Green, E.C., 2017. High-grade metamorphism and partial melting in Archean composite grey gneiss complexes. J. Metamorph. Geol. 35,
- Whitney, D.L., Evans, B.W., 2010. Abbreviations for names of rock-forming minerals. Am. Mineral, 95, 185-187.
- Yakymchuk, C., Brown, M., 2014. Consequences of open-system melting in tectonics. J. Geol. Soc. 171, 21-40.

JID:EPSL AID:118405 /SCO ARTICLE IN PRESS [m5G; v1.343] P.12 (1-11)

Appendix A. Supplementary material The following is the Supplementary material related to this article. **bugin accomponent bugin accomponent and acco

link: APPLICATION:mmc2

Sponsor names

Do not correct this page. Please mark corrections to sponsor names and grant numbers in the main text.

Natural Sciences and Engineering Research Council of Canada, country=Canada, grants=

National Science Foundation, country=United States, grants=EAR 2022746

[m5G; v1.343] P.14 (1-11) JID:EPSL AID:118405 /SCO

Highlights

- Europium anomalies of zircon are modelled for metamorphic and igneous systems.
- \bullet Eu anomalies in zircon vary with rock type, temperature, pressure, and f_{02} .
- Zircon Eu anomalies are not an appropriate proxy for crustal depth.
- Secular change of zircon Eu reflect variations in P/T or crustal reworking.